

An investigation of a dramatic cold outbreak over southeast Australia

Ian Simmonds and Harun A. Rashid*

School of Earth Sciences, University of Melbourne, Victoria, Australia

(Manuscript submitted April 2001; revised August 2001)

This paper investigates an episode of three successive cold outbreak events that took place over southeast Australia during May-June 2000. Of these three cold events, the most intense occurred on 27-28 May and was associated with a Melbourne maximum temperature of only 10.2°C. This is the second lowest daily maximum temperature recorded in Melbourne for May since 1958. The other two events, with slightly higher daily maximum temperatures, followed the first event closely. Various data processing techniques along with an air-parcel trajectory model and a sophisticated vortex tracking scheme are utilised to examine several aspects of these cold events, with a particular emphasis on the major event of 27 May.

Results show that the synoptic pattern and its temporal evolution leading to the major event were characterised by a persistent anticyclone-cyclone dipole, located south of Australia. On the onset day, the configuration and position of this anticyclone-cyclone pair was such that a strong cold advection from the interior of Antarctica was implied, which was confirmed by computing air-parcel trajectories at the 1000 hPa level. Of the anticyclone and cyclone, the former was found to have a dominant influence on the occurrence and evolution of cold outbreaks over southeast Australia. This was demonstrated by analysing the tracks and the changes in intensity, 'height', and effective radius of the anticyclones that were associated with two of the three outbreak events. Analysis shows that the anticyclones, which were in rapid translational motion initially, became quasi-stationary near southern Australia during the later stages of their lifecycles. At these times, the anticyclones also strengthened significantly, as revealed by increases in their intensity, height, and effective radius.

Analyses of the 500 hPa height field show that the above anticyclone-cyclone pair was indeed a part of a large-amplitude hemispheric wave train with a remarkable degree of structural organisation. Much of this organisation was due to the amplification of wavenumber 4 prior to the onset of the cold events. Initially, the wave energy was concentrated mainly in the eastern hemisphere. However, concurrent with the decay of the first cold event, the energy propagated downstream very quickly, resulting in an amplified wave train in the western hemisphere. This downstream wave development was found to continue for an unusually long time, making two revolutions around the hemisphere and, also, triggering two of the three cold outbreak events studied in this paper.

Introduction

Extremely cold days with temperatures well below normal are found to occur in the southern parts of

Australia, as in some other places of the world (Perrin and Simmonds 1995; Wu and Chan 1997; Lagouvardos et al. 1998; Schultz et al. 1998; Garreaud 2000; Simmonds and Richter 2000; Vera and Vigliarolo 2000; Xue et al. 2000; Pagowski and Moore 2001; and references therein). These cold

Corresponding author address: Dr Ian Simmonds, School of Earth Sciences, The University of Melbourne, Vic. 3010, Australia.

*Permanent affiliation: Department of Physics, University of Chittagong, Chittagong, Bangladesh.

weather events are characterised by a rapid fall in temperature and, sometimes, by an equally rapid rise in pressure in the affected region (e.g., Colle and Mass 1995). They are usually of short duration (2-5 days) and tend to be associated with characteristic synoptic patterns. The frequency of their occurrence varies widely depending on the geographic location and, to some extent, on season. However, irrespective of their frequency of occurrence, these severe weather events can create a significant impact on the economic and social aspects of the affected regions (e.g., Marengo et al. 1997). Moreover, they are responsible for bringing about considerable disruption in everyday activities of the people living in the regions where they occur. As a result, the cold outbreak events, as they are often called, have attracted widespread attention of atmospheric scientists all over the world.

Different approaches to investigate cold outbreak events have been employed by various investigators in an attempt to understand the physical mechanisms involved. A significant number of previous studies have adopted synoptic approaches, often complemented by diagnostic and modelling studies, to describe the circulation features and weather conditions associated with cold outbreaks concentrating on a small number of events (e.g., Schultz et al. 1997; Krishnamurti et al. 1999). Others have used compositing procedures, again sometimes complemented by other techniques, to determine the mean structure and evolution of these severe weather events (e.g., Konrad 1998; Schultz et al. 1998; Simmonds and Richter 2000). The pictures concerning the structure and dynamics of cold outbreaks that come out of these various investigations have both common and differing components. For example, the effects of downstream amplification of synoptic-scale weather systems and associated energy propagation have been reported to be important for the occurrences of cold outbreaks over regions as widely separated as South America (Fortune and Kousky 1983; Krishnamurti et al. 1999), North America (Orlanski and Sheldon 1995) and East Asia (Joung and Hitchman 1982). On the other hand, in studying cold outbreaks over North and Central America, Colle and Mass (1995) and Schultz et al. (1997) found the important role played by the Rocky Mountains in determining the character of the outbreak events there. However, in the east Asian region, the cold surges are mainly characterised by the passage of short waves through the existing long wave trough there (Boyle 1986). Similarly, while the Andes Mountains have a prominent role in the occurrences of cold outbreaks over South America (Marengo et al. 1997; Garreaud 2000), such topographic factors may not be of importance to the cold

outbreak events over the Australian region. It is therefore obvious that cold outbreak events over different geographic locations and at different times of the year need separate investigations to fully comprehend their structure and dynamics.

Cold outbreaks over the Australian region have been previously studied by a number of investigators (Hannay 1960; Taylor and Stern 1982; Pook 1992; Perrin and Simmonds 1995; Simmonds and Richter 2000; Jones, private communication). Most of these studies considered the mean structure and evolution of a number of cold outbreak events using compositing techniques. Perrin and Simmonds (1995) utilised daily maximum temperature observations for Melbourne and daily hemispheric numerical analyses, both obtained from the Australian Bureau of Meteorology, to analyse the cold outbreak events that occurred in Melbourne over the period 1972-1991. They identified cold outbreak days as those on which the daily maximum temperature fell below the corresponding monthly mean value by more than two standard deviations. Applying this criterion, they identified a total of 13 cold-outbreak events during their study period, most of which, however, fell in the winter season (June, July and August). Perrin and Simmonds (1995) carried out a synoptic classification based on these 13 cases, and identified three categories of cold outbreaks: classic, warm front and blocking anticyclone type. The classic type outbreaks were most prevalent, consisting of an anticyclone-cyclone pair with the anticyclone being positioned upstream and the cyclone downstream. Later, Simmonds and Richter (2000) modified the outbreak identification criterion to remove the strong seasonal bias present in the number of identified outbreak events in Perrin and Simmonds (1995). Extending the work of Perrin and Simmonds (1995), they considered the Melbourne cold outbreak events for summer and the Perth events for both summer and winter over the same 1972-1991 period. In this later study, features of cold outbreaks over Melbourne versus Perth and also for summer versus winter were contrasted to gain a deeper understanding of the outbreak events occurring in the southern Australian region. The classic type events were again found to be the most commonly occurring type in both the cities and in both seasons, with a characteristic composite synoptic pattern comprising an upstream anticyclone and a downstream cyclone. The relative importance of the two features of the anticyclone-cyclone pair in relation to the cold events was, however, found to be different for Melbourne and Perth. While the anticyclone dominated the composite synoptic structure for Melbourne, the reverse was true for Perth. Differences based on seasons were also reported.

While composite studies, such as discussed above, reveal useful information about the mean structure and evolution of typical cold events, it is also useful to consider aspects of individual events separately, especially when the events exhibit very anomalous behaviour. In this paper, we employ this latter approach to investigate a series of three successive cold outbreaks that took place between 26 May–13 June 2000 (hereafter referred to as the MJ2000 episode) over southeast Australia. These cold events were unusual in a number of respects. The first of these three events made onset on May 27 and had associated with it the second lowest daily maximum temperature for May since 1958. In addition, southern Australia and the adjacent ocean area had been under the influence of a mean sea-level pressure high throughout the lifetime of the MJ2000 episode, a period long compared to typical anticyclone lifecycles. Given these unusual characteristics, we believe that a thorough investigation of different aspects of the MJ2000 episode will further our present understanding of the cold outbreaks gained through the past composite studies. With this motivation in mind, we in this study:

- analyse the synoptic situation in which the major cold outbreak of 27 May took place, and compare the results with those of previous composite studies;
- investigate in detail the role played by anticyclones in giving rise to the sequence of cold outbreaks using a sophisticated (anti)cyclone finding scheme;
- and examine the possible relationship between the cold outbreaks in the Australian region and some aspects of the planetary-scale circulation field, namely wave number characteristics and downstream baroclinic development, which were not considered before in any detail for this region.

This paper is organised as follows. The first section describes the datasets used and outlines the preliminary processing. In the next section, the synoptic aspect, upper-level circulation features, and the structural evolution of the major cold outbreak event are discussed in detail. An analysis of the tracks and strength of the associated anticyclones is also presented in this section. Wavenumber characteristics of the large-scale, upper-level circulation along with the downstream propagation of the associated wave energy are described in the following section. Finally, we summarise the main results of the study.

Data and preliminary analysis

In the present work, we have utilised the National Centers for Environmental Prediction – National

Center for Atmospheric Research (NCEP-NCAR) Reanalyses for May and June 2000. The dataset comprises global, gridded analyses on a $2.5^\circ \times 2.5^\circ$ latitude-longitude grid at six-hourly intervals. Details of the NCEP-NCAR Reanalyses project and the data quality may be found in Kalnay et al. (1996) and Kistler et al. (2001). In using the NCEP-NCAR Reanalyses for southern hemisphere (SH) studies one should be aware of the problems that may be associated with these Reanalyses arising from a number of causes (e.g., see Kistler et al. 2001), including the misplacement of the Australian surface pressure bogus data (PAOBS) between 1979 and 1992. During this period the bogus data were incorrectly shifted by 180° longitude before being assimilated (see, e.g., Seaman et al. 1993). The impacts of this mislocation on the accuracy of the southern hemisphere Reanalyses were assessed by NCEP-NCAR (details about this assessment may be found at the NCEP Web site at <http://wesley.wv.noaa.gov/paobs/paobs.html>). Briefly, the results of their assessment indicate that the region most affected by this error lies south of about $40\text{--}60^\circ\text{S}$ and that the magnitude of the error decreases rapidly as the time-scale increases from synoptic to monthly. Simmonds and Keay (2000) conducted additional assessments in this regard and showed that, despite these problems, reliable and robust climatologies of cyclone tracks in the SH can be constructed from the Reanalyses. The PAOBS problem does not, however, directly affect our present study, as the cold outbreaks being investigated here occurred in May–June 2000. The only connection this study may have to the PAOBS problem is through our use of the 40-year (1958–97) NCEP-NCAR monthly climatologies. This, too, should not affect the results presented here in any significant way, as the PAOBS problem has minimal consequences for monthly means and, also, as the PAOBS-affected reanalyses represent only approximately one-third of the reanalyses from which the climatologies were computed.

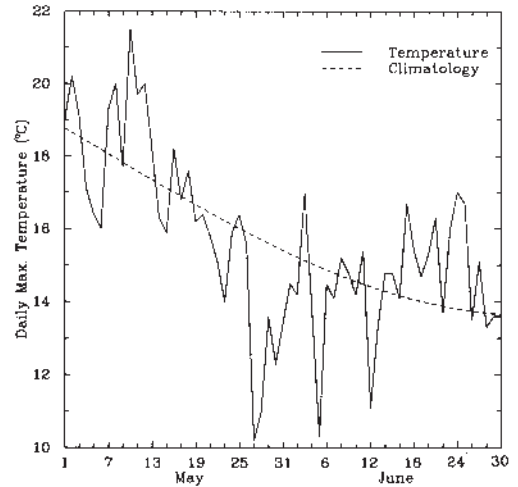
We have used for our work geopotential height analyses at the 500 and 300 hPa levels, and mean sea-level pressure (MSLP). The zonal and meridional velocity components at the 1000 and 850 hPa levels have also been used. In order to calculate anomalies, we have utilised the 40-year (1958–97) NCEP-NCAR monthly mean climatologies for MSLP and 500 hPa height. Computing daily anomalies simply by subtracting the monthly means from daily data, as is done in many cases, is not appropriate in our case. The cold events we examine here extend over a period of about three weeks, and this period is long enough for the (daily) climatological values to change significantly. Therefore, the daily anomalies computed using the above procedure

would contain a changing component due to the climatological annual variation as well as the short-term variations contributed by the cold outbreaks. This climatological component would appear as a trend in the computed anomalies over the MJ2000 episode, masking, at least partially, the cold event induced variability. To overcome this difficulty, we have first estimated the daily climatological values from the monthly mean climatologies using the spectral (Fourier) interpolation technique. The interpolation is accomplished by expanding the monthly mean data in Fourier series and then inverse transforming to daily values using an appropriately reduced time interval, retaining only the time-mean and the first four harmonics (12, 6, 4 and 3-monthly harmonics). The daily anomalous values for MSLP and 500 hPa are then obtained by subtracting the respective daily climatological values from 0000 UTC MSLP and 500 hPa analyses for each day of May-June 2000.

Synoptic structure and evolution

As mentioned in the Introduction, the first of the three cold outbreaks in the MJ2000 episode took place on 27-28 May 2000. After this, two somewhat less intense outbreak events were also recorded in close succession: one on 5 June and the other on 12 June 2000. These cold events can be identified in the time series of daily maximum temperatures observed in Melbourne for the period 1 May-30 June 2000 (Fig. 1). The first, major event on 27 May recorded a daily maximum temperature of only 10.2°C, 6.8°C below the long term average value (17.0°C) for May. As noted earlier, this is the second lowest daily maximum temperature for May since 1958. The second cold event on 5 June trailed the first event only by a small difference in observed daily maximum temperature, recording a value of 10.3°C. The departure of daily maximum temperature in this case from the long term June averaged value (14.4°C) is -4.1°C. For the third cold event on 12 June the observed daily maximum temperature was 11.1°C, with a departure of -3.3°C from the long-term June averaged value. When calculated as deviations from the corresponding long term daily-averaged (i.e., daily climatological) values, the respective departures become -5.6°C, -4.7°C, and -3.3°C. The falls in observed maximum temperature from the previous days' maxima for the above three cold events are 5.4°C, 3.5°C, and 4.3°C, respectively. During the whole MJ2000 episode, the maximum temperatures remained below the corresponding climatological values, except for four days.

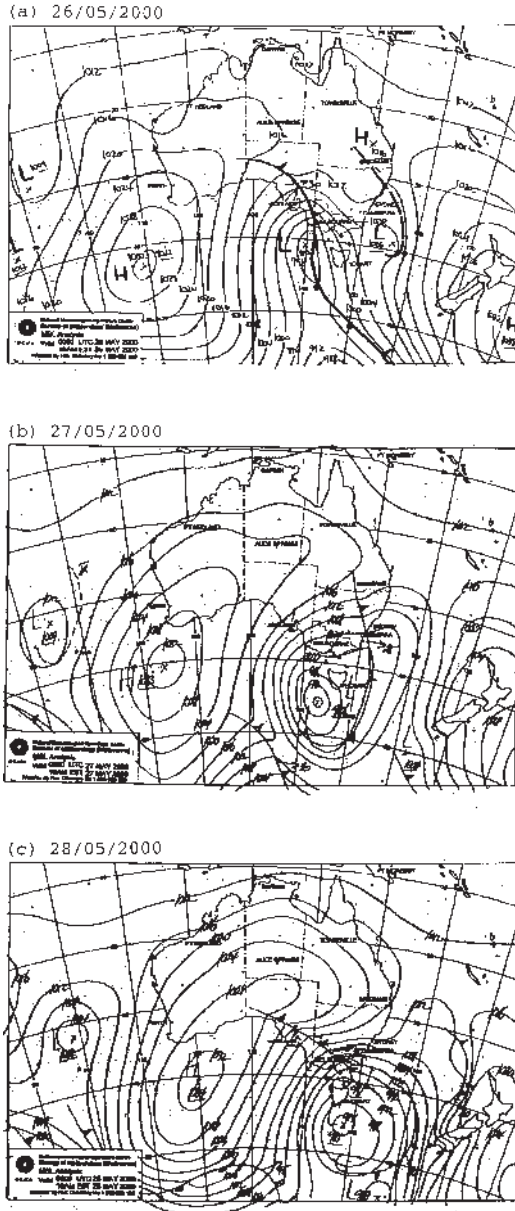
Fig. 1 Time series of daily maximum temperatures (°C) at Melbourne for the period 01 May-30 June 2000 (solid line). Also shown in the Figure are the daily climatological values (dashed line) of daily maximum temperature for the same period.



Synoptic situation

Although the lowest daily maximum temperature during the MJ2000 episode occurred on 27 May, the following day was also very cold, with a maximum temperature of only 11.0°C. Figure 2 shows the mean sea-level pressure (MSLP) analyses charts from the Bureau of Meteorology valid at 0000 UTC 26, 27 and 28 May (parts a, b and c). The charts are dominated by an intense high pressure system with central pressures of about 1033 hPa. On May 26, the anticyclonic system is centred to the southwest of Australia. To the east of this system is located a low pressure system, with a central pressure of 990 hPa, just west of Tasmania. This particular configuration of the anticyclone-cyclone pair is characteristic of 'classic' type events found by Perrin and Simmonds (1995) and Simmonds and Richter (2000). As in the classic-type events of these previous studies, an analysed cold front is seen to be associated with the cyclonic system, which has a predominantly north-south orientation on 26 May. The following day, on which the lowest daily maximum temperature was recorded, the front sweeps across Victoria. The synoptic pattern remains almost the same as that on the previous day, except that the anticyclone has now shifted slightly to the northeast and the cyclone to the southeast. Also, the cyclone has deepened somewhat with the central pressure now falling to 986 hPa. The whole pattern moves still further east on May 28. Moreover, both

Fig. 2 Analysed mean sea level pressure charts for (a) 26 May, (b) 27 May and (c) 28 May 2000, valid at 0000 UTC each day. Contour interval is 4 hPa. The high and low pressure centres are shown by letters 'H' and 'L', respectively. Analysed cold fronts are also shown.



components of the anticyclone-cyclone pair have strengthened even further, reaching their extreme values (1034 and 981 hPa, respectively) for this cold event. A peculiar feature of the synoptic chart of May 28 is that a cold front is now seen to be situated over

Victoria, while the cold front on the previous day was located farther east. (The MSLP distribution from NCEP-NCAR Reanalyses (not shown) also shows similar kinks in the isobars, implying the existence of a cold front approximately at the same position.)

The sequence of the synoptic charts discussed above points to the central role played by an intense anticyclone-cyclone pair, located south of Australia, in the occurrence of the cold outbreak event of 27 May. These weather systems were conducive to establishing a strong surface southwesterly wind that advected the very cold polar air northward up to southeast Australia. To confirm this, we have performed a six-day backward trajectory analysis of the air parcels reaching Melbourne for each day of the period 25-30 May. The fourth order Runge-Kutta trajectory model developed by Law (1993) and described in Perrin and Simmonds (1995) is used in the analysis. The six-day trajectories calculated from the 1000 hPa horizontal wind fields are shown in Fig. 3(a). It is seen that for those air parcels reaching Melbourne prior to the cold outbreak the trajectories originated at nearby regions around Melbourne. However, for the air parcels arriving at Melbourne on the day of the cold outbreak onset, the trajectory emanated from the deep polar region (-77.8° latitude and 118.7° longitude) six days before its arrival at the destination. In this case, the trajectory is oriented in a more or less north-south direction, signifying a quick travel from the Antarctic interior to over Melbourne. For the subsequent days, the air parcels coming to Melbourne had originated at source regions situated progressively further north. It is therefore clear that the cold outbreak event of 27 May was initiated by the advection of very cold air from inland Antarctica under the influence of the anticyclone-cyclone pair discussed above.

To examine the reliability of these calculated air-parcel trajectories, we carried out a stability analysis of the trajectories by first choosing a number of arrival points on a square grid around Melbourne and then determining the corresponding source locations. The square grid chosen is of 1° width in north-south and east-west directions. The result for 27 May is presented in Fig. 3(b) and Table 1. The average distance between all possible pairs of points in the arrival region is 81.56 km; the corresponding figure for the points in the source region is 183.4 km, giving a ratio of 1:2.25. That is, the average distance between the trajectories at the source region is increased by a factor of a little over two over the six-day period considered. Considering that we are concerned with source regions rather than source points, the above trajectory analysis gives a reasonably accurate description of the air-parcel trajectories and their origins.

Fig. 3(a) Six-day air-parcel trajectories arriving in Melbourne at 1000 hPa level for each day of 25 May-30 May 2000. The trajectories are marked with the travel dates of the corresponding air-parcels. For each day, the trajectory started at a date six days before the respective date of arrival at Melbourne.

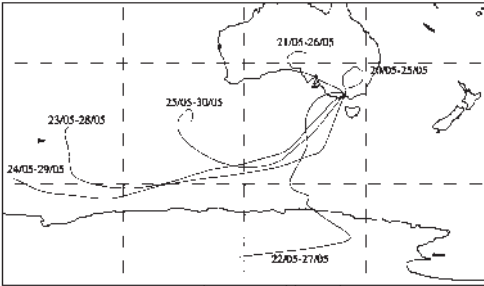


Fig. 3(b) Six-day air-parcel trajectories arriving at a number of nearby points around Melbourne on 27 May 2000. The arrival points were chosen to be located on a $1^\circ \times 1^\circ$ grid centred at Melbourne.

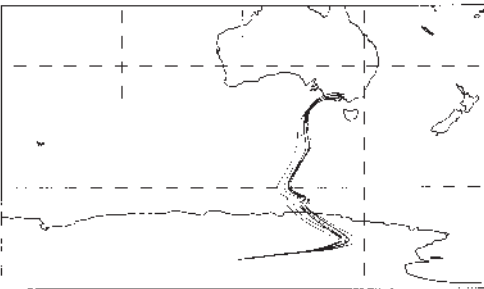


Table 1. Source locations of different air-parcel trajectories arriving at different locations around Melbourne on 27 May.

Source locations		Arrival locations	
Lat. (deg.)	Long. (deg.)	Lat. (deg.)	Long. (deg.)
-77.36	121.68	-37.32	144.47
-76.91	125.12	-37.32	144.97
-75.96	134.86	-37.32	145.47
-77.37	121.46	-37.82	144.47
-77.76	118.73	-37.82	144.97
-77.53	120.57	-37.82	145.47
-76.26	130.27	-38.32	144.47
-77.53	120.21	-38.32	144.97
-77.99	117.22	-38.32	145.47

Upper-level circulation

To display the upper-level circulation features associated with the cold outbreak event, hemispheric maps of 500 hPa height for 27 and 28 May 2000 are presented in Fig. 4. The distribution on 27 May (Fig. 4(a)) shows a well-developed wave train encircling the hemisphere in the extratropics. The wave pattern in the eastern hemisphere (i.e., upstream of Melbourne) is clearly better organised than that in the western hemisphere. The waves attain their maximum amplitudes at around 55°S latitude. As will be shown later, this wave pattern has a pronounced wavenumber 4 structure. Of particular interest for our present work is the anticyclone-cyclone pair located just south of Australia. These systems are shifted somewhat to the west with respect to their surface counterparts, an orientation typical of the mid-latitude baroclinic systems. The wave structure remains much the same through the next day (Fig. 4(b)), with an eastward progression of the wave train in the Indian Ocean sector. It is interesting to note that the strongest anticyclone, which on the previous day was positioned east-southeast of New Zealand, has now moved south-westward to be centred just west of the date-line. Furthermore, this system remained quasi-stationary at that location for a few more days, producing a blocking effect for the anticyclone-cyclone pair upstream at the Australian sector. At the same time, the hemispheric wave pattern continued to show a good deal of organisation until June (not shown), after which the pattern began to break down.

The hemispheric distributions of height at 300 hPa (not shown) show patterns much the same as those at 500 hPa, with wave amplitudes at the former level being somewhat larger and with very little, if any, westward phase-tilts.

Time evolution

It is important to see how the mobile high and low, constituting the anticyclone-cyclone pair mentioned above, evolved prior to and after the onset of the cold event. In Fig. 5, we present a sequence of maps showing the anomalous MSLP distributions over the period 23-30 May. On 23 May, the distribution of MSLP anomalies (Fig. 5(a)) shows a broad low pressure area, with two discernible centres over the Southern Ocean south and southeast of Australia. At that time the anticyclone is seen to be positioned to the west near 90°E . During the next 24 hours (Fig. 5(b)), one of the two low pressure centres comes closer to the anticyclone while, at the same time, getting stronger. The anticyclone also moves somewhat to the east. By May 25 (Fig. 5(c)), the anticyclone and the cyclone become very well-structured with a slight weakening of the former and strengthening of the latter. Over the

Fig. 4 Hemispheric distributions of 500 hPa geopotential height (m) for (a) 27 May 2000 and (b) 28 May 2000. Contour interval is 100 m. Highs and lows are marked with letters 'H' and 'L', respectively.

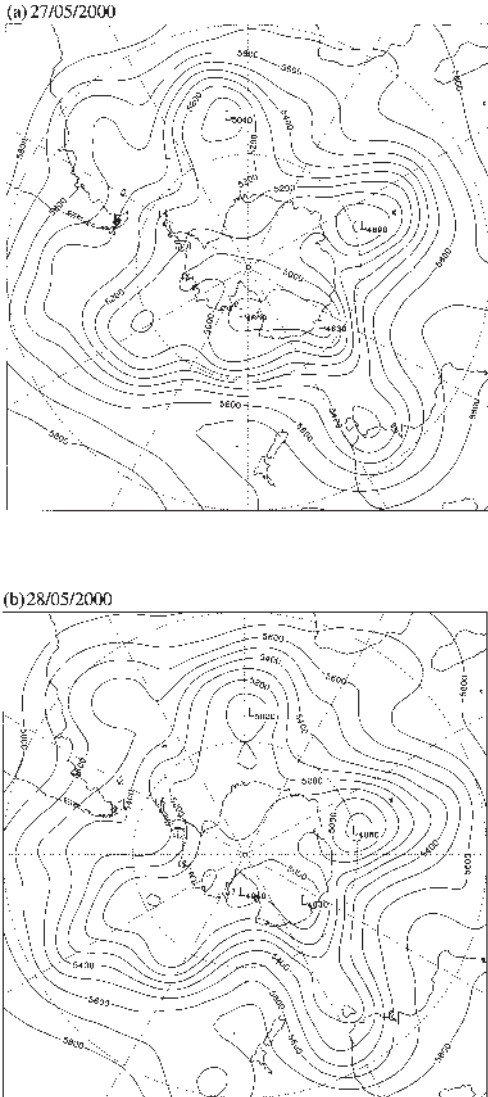
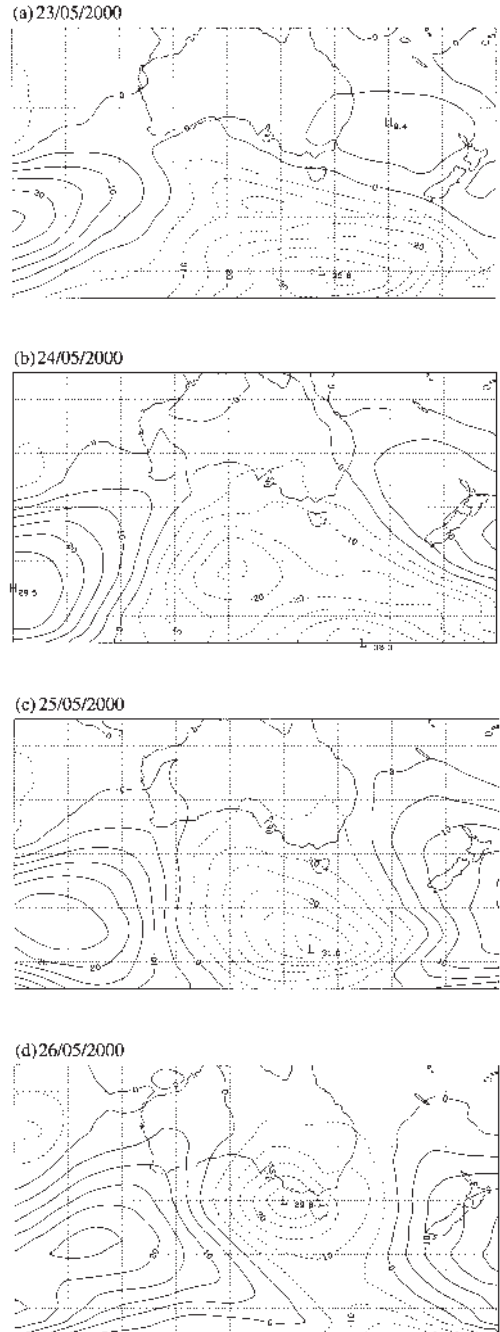
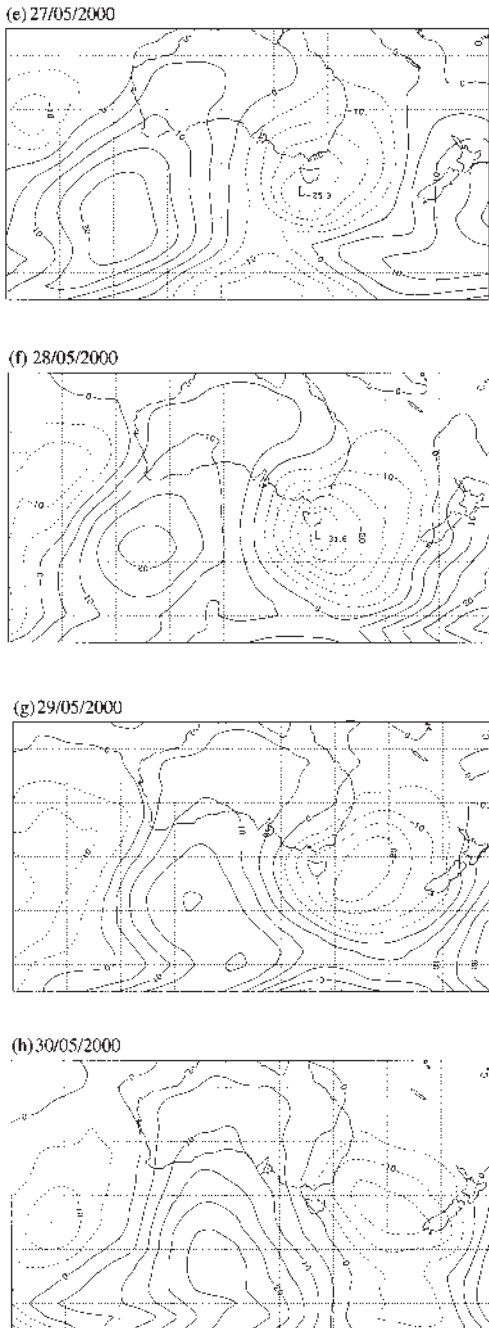


Fig. 5 Anomalous MSLP (hPa) distributions in the Australian region around the major cold-air outbreak date (27 May 2000): (a) 23 May, (b) 24 May, (c) 25 May, (d) 26 May, (e) 27 May, (f) 28 May, (g) 29 May and (h) 30 May. Contour interval is 5 hPa. Positive (negative) anomalies are contoured with solid (dashed) lines.



next two days (Fig. 5(d), (e)), both systems get weaker with the anticyclone moving slightly towards the northeast. However, during the first half of this period the cyclone shifts northward by a large distance, in excess of about 15° latitude, to be centred just south of Victoria. At this stage, the configuration of the anticyclone-cyclone pair and their positions relative to southern Australia are ideal for the polar air advect-

Fig. 5 Continued.



tion, discussed earlier, to take place. It may be noted that, on the coldest day (27 May), neither of these two systems were at their peak strengths, although they were strong enough to cause a significant cold air

advection. In the present case, the factors that appear to be more important for leading to the cold outbreak are their mutual configuration and their positions relative to the affected region. This configuration of the anticyclone-cyclone pair is seen to be maintained during the subsequent days (Fig. 5(f), (g), (h)), while the pair continues its eastward propagation.

Anticyclone tracks and strength

Considering the key role played by the anticyclone-cyclone pair in initiating the cold outbreak event of 27 May, it is important to have a more quantitative understanding of the movement, intensification, and 'size' of these synoptic-scale weather systems. In particular, a quantitative examination of the behaviour of the anticyclone, which tends to show a better organisation than the cyclone, over its lifetime may provide further insight into the mechanism of the cold outbreak. Focusing on the anticyclone is consistent with the fact that Simmonds and Richter (2000) found the role of the anticyclone to be more important than the companion cyclone in the evolution of the 'classic' type outbreak events occurring in Melbourne. Some other studies (Konrad and Colucci 1989; Roggers and Rohli 1991; Konrad 1996) also reported that strong cold outbreaks are more controlled by the strength of the upstream anticyclone than by the downstream cyclone. To carry out the present analysis, we use a sophisticated, objective cyclone finding and tracking scheme developed at the University of Melbourne (Murray and Simmonds 1991; Simmonds et al. 1999). This cyclone finding scheme can be adapted to use in anticyclone finding and tracking by merely a sign change in the corresponding computer code. This scheme has been used in a number of previous studies to construct comprehensive climatologies for southern hemisphere extratropical cyclones and anticyclones using MSLP analyses (Jones and Simmonds 1993, 1994; Simmonds and Keay 2000).

Figure 6(a) shows the tracks of two anticyclonic systems that were in the Australian region at around the time of the cold outbreaks. The zonal displacements of the two systems as a function of time over their lifecycles are also displayed in Fig. 6(b). Both of these anticyclones were very long-lived (21 and 17 days, respectively) and spent a considerable time in the Great Australian Bight. The first anticyclone (shown by the solid line) developed west of the Greenwich Mean line at 1800 UTC 12 May and travelled a long distance over the Southern Ocean before it reached near southwest Australia around 26 May, shortly before the onset of the first cold outbreak. Subsequently, the track of this anticyclonic system became more erratic with slow back and forth movements in the Bight region mainly in the north-south

Fig. 6(a) Tracks of two anticyclones involved in the two cold-air outbreak events during the MJ2000 episode. The track of the first anticyclone (solid line) starts at 1800 UTC 12 May and ends at 0600 UTC 2 June, while the track of the second anticyclone (dashed line) starts at 1200 UTC 31 May and ends at 0600 UTC 17 June. Four times daily data were used to calculate the tracks. The first anticyclone showed characteristic temporal evolution during the major cold-air outbreak event of 27 May. Similar temporal evolution was shown by the second anticyclone around the time of the cold-air outbreak event of 12 June.

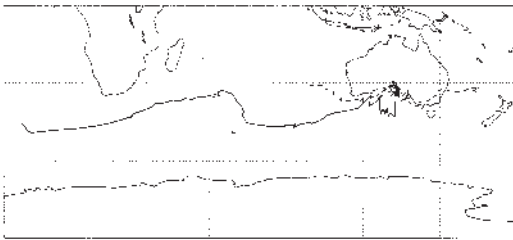
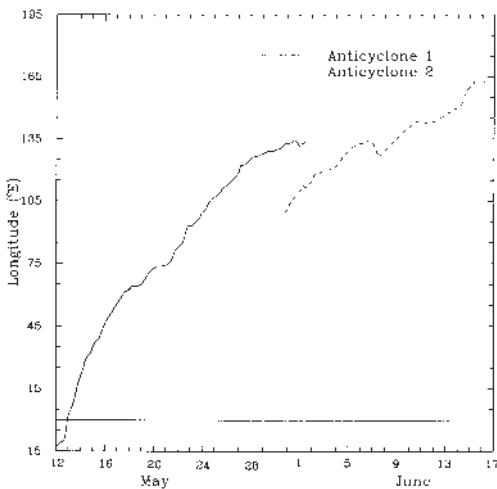


Fig. 6(b) Longitudinal positions (°E) of the two anticyclones as a function of time during their lifecycles.

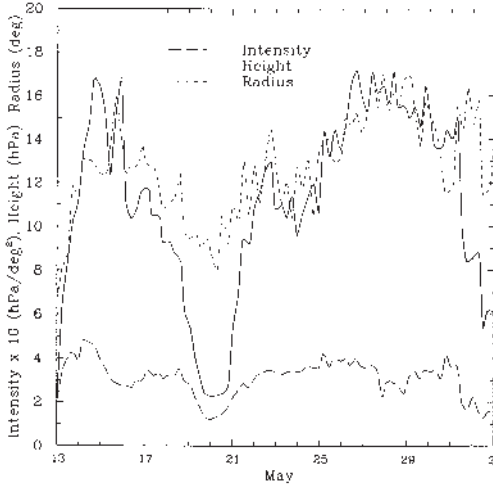


direction (Fig. 6a). After spending more than a week in this region, the system finally dissipated over South Australia at 0600 UTC 2 June. Meanwhile, a second high-pressure system (represented by the dashed line) developed over the subtropical eastern Indian Ocean at 1200 UTC 31 May, two days before the decay of the first system. This second anticyclone also exhibit-

ed a very slow translational motion, and followed a path close to the coastline of southern Australia. After spending most of its lifetime in the Australian sector, the anticyclonic system decayed over the Tasman Sea at 0600 UTC 17 June. As is evident from Fig. 6(b), the paths followed by these two separate systems along with the timing of their movements were such that the dissipation of the first system over the Bight was almost immediately followed by the arrival there of the second high pressure system. Therefore, around and after the major outbreak event of 27 May the synoptic condition over the Southern Ocean in the Australian sector continued to be characterised by a prolonged presence of anticyclonic systems. This is critical to the occurrences of two more minor cold outbreaks within a short time-span after the major outbreak event of 27 May.

The anticyclones also show interesting features in the time evolutions of their intensity, ‘height’ and effective radius over the respective lifecycles. Simmonds and Keay (2000) discuss in detail how these parameters, taken together, represent a comprehensive measure of the strength of extratropical cyclones and their influence on the climate maintenance. The same concepts, with appropriate definitions of the parameters, apply to mobile anticyclones as well. The intensity of an anticyclone is defined as minus the Laplacian of the pressure field calculated at the centre of the systems ($-\nabla^2 p_c$) (e.g., Bluestein 1992) and the ‘height’ as the pressure difference between the centre and the ‘edge’ of the anticyclone. We present in Fig. 7 the time series plot of these parameters along with effective radius (a measure of the size of the system) for the first anticyclone over its lifetime (1800 UTC 12 May-0600 UTC 2 June). The temporal variations of the three quantities show similar patterns. Shortly after its formation, the anticyclone grew in size, intensity, and height quite rapidly, approaching the respective local maxima around 13-15 May. It then decayed as rapidly to reach the minima around 20 May. At the same time, the anticyclonic system underwent a northward migration over the Indian Ocean (cf. Fig. 6(a)), reaching as far north as 32°S. It may be noted that the variations in intensity tend to precede the similar variations in the other two quantities. After a period of minimum strength, the anticyclone again experienced a rapid increase in its intensity, height, and size after 20 May. The system reached its peak strength, defined in terms of the above quantities, just before May 27. During the lifetime of the major outbreak (27-28 May) and afterwards, the anticyclone continued to exhibit maxima in height and size with some small day-to-day fluctuations. However, as before, the intensity has a tendency to reach its maximum value when the other two

Fig. 7 Time series plots of intensity (hPa/deg^2), 'height' (hPa), and effective radius (deg. latitude) for the first anticyclone (1800 UTC 12 May-0600 UTC 2 June). For clarity, the intensity values were multiplied by 10 before plotting.



quantities are still increasing in magnitude. Subsequently, after a period of more gradual decrease, the height and intensity of the anticyclone diminished more rapidly before it dissipated on 2 June. A similar timeseries plot (not shown) was also prepared for the second anticyclone. The temporal behaviour of the strength of the system showed much the same pattern as that of the first system in relation to the cold outbreak onset. However, the maxima around 5 June, the date of the second cold outbreak, are not as prominent as those around 12 June, the date of the third cold outbreak. This suggests that the second anticyclone has more to do with the cold outbreak event of 12 June than with that of 5 June.

The above analysis of the anticyclone track, residence time in the Bight, and the temporal behaviour reinforces the key role played by the anticyclonic system in causing the cold outbreak events, especially those of 27 May and 12 June.

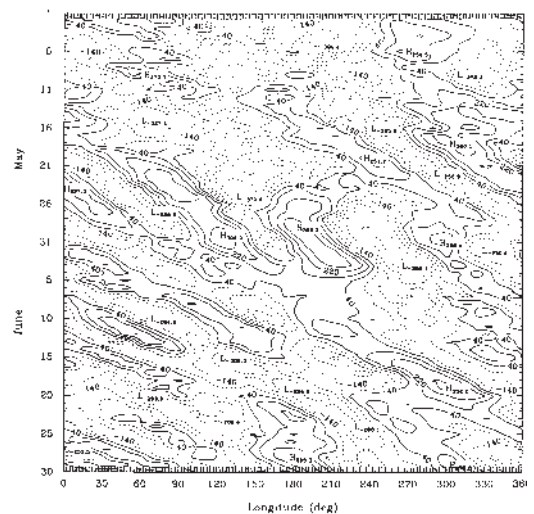
Relationship with planetary-scale waves

As discussed in a previous subsection, the large-scale circulation field around and on the cold outbreak day was dominated by a hemisphere-wide, well-developed wave pattern, and the anticyclone-cyclone pair

responsible for the outbreak was a part of that wave train. Therefore, in understanding the dynamics of the cold outbreak event, it is important to examine the time development and phase propagation of these waves to explore links between the planetary-scale wave propagation and the cold events. A suitable analysis tool for depicting temporal developments of wave patterns, their phase propagation, as well as estimating the group velocity is the Hovmöller diagram (Hovmöller 1949). Figure 8 shows such a diagram of 500 hPa height anomalies at 55°S for the period 1 May-30 June, 2000. Ridges and troughs with considerable amplitudes are seen to propagate in a predominantly eastward direction. Of particular relevance to the present work is the ridge-trough system which arrives in the Australian sector (~ 110 - 150° longitude) at approximately the same time as the first cold outbreak onset (27 May). It is clear from the figure that the ridge of this system propagated a long way through the South Indian Ocean, and attained significant amplitudes in the later stages of this propagation, before reaching the Australian sector. From about 2 June onward, the amplitudes of the waves throughout the hemisphere reduce considerably, with the above-mentioned ridge still showing a discernible eastward propagation.

The enhanced wave activity before and after the major cold outbreak event discussed above appears to have played a crucial role in causing the event. In order to isolate the contribution from the individual

Fig. 8 Hovmöller diagram (x - t) of 500-hPa height anomalies (m) at 55°S latitude for the period 1 May-30 June 2000. Positive (negative) anomalies are shown by solid (dashed) contours. Contour interval is 90 m.



wave components, we compute the amplitudes of zonal wavenumbers 0-5 by decomposing the height anomalies at 55°S over the same two-month period as above. Only the wave amplitudes for wavenumbers 4 and 5 are shown in Fig. 9, as the other waves do not exhibit any characteristic behaviour during the outbreak events. Inspection of Fig. 9 shows the large amplitude associated with wavenumber 4 over a period surrounding the cold outbreak day. This wave undergoes a rapid amplification after 17 May, reaching its maximum amplitude on 25 May and then decaying briefly. It is during this temporary decay period for wave 4 that the outbreak occurs. The wave 4 amplitude continues to decrease following the outbreak onset date until May 29, after which date the wave again starts to amplify. It is interesting to note that the second and third cold outbreak events in the MJ2000 episode (on 5 and 12 June) are also accompanied by such a temporary decrease in wave 4 amplitude following an amplification of the same prior to the events. As noted above, no other waves show any noticeable amplification during the outbreak periods, except a minor increase in the amplitude of wave number 5 with its highest value occurring on 28 May.

The above analysis gives a clear indication of the involvement of wavenumber 4 and, to a lesser extent, wavenumber 5 in the occurrence of the cold outbreak events during the MJ2000 episode. To reveal the phase propagation and longitudinal variation of amplitudes associated with these waves, we present in Fig. 10 the Hovmöller diagram constructed from height anomalies filtered to retain only these two waves. Consistent with Fig. 9, large amplitude values, mostly contributed by wave 4, are seen to occur over periods extending from a few days before the outbreak events to a few days after the events. In addition to the phase propagation, there is also a clear indication of the eastward propagation of the wave group and associated wave energy with time. For example, on 25 May the wave group is more energetic over the eastern hemisphere than over the western hemisphere. About one week later, on 31 May, the wave group is much more prominent in the western hemisphere, suggesting a significant downstream development of the wave group and associated energy over the interval between 25 and 31 May. A similar downstream development is observed during the period 10 June to 15 June. It may be noted that the cold outbreak events of 27 May and 12 June occurred during the times of the downstream developments mentioned above. However, such a relationship between cold outbreak and downstream development of the wave group is not apparent for the outbreak event of 5 June. A closer examination of Fig. 10 reveals that the process of

Fig. 9 Time series plots of the wave amplitudes of 500 hPa height anomalies (m) for wavenumbers 4 and 5 at 55°S latitude over the period 1 May-30 June.

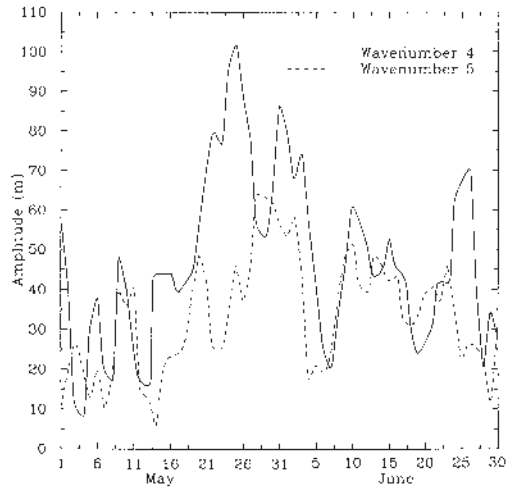
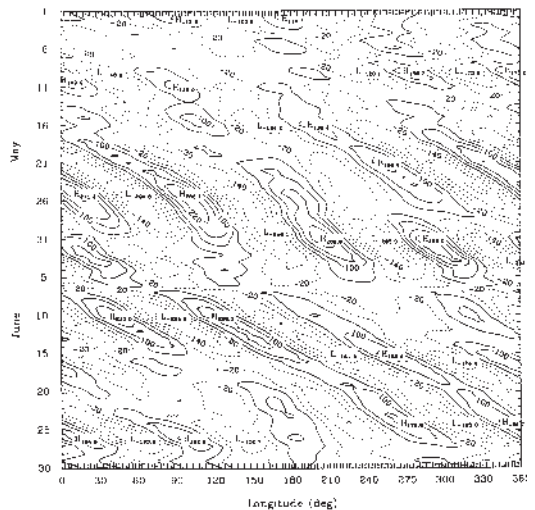


Fig. 10 Same as Fig. 8, but for height anomalies filtered to retain only wavenumbers 4 and 5. Contour interval is 60 m.



downstream development was actually going on for a longer time and over a larger distance than might appear at first instance. The process starts at around 21 May with a pair of ridge-trough systems developing between 240°E and 300°E, and then continues for a considerable length of time, travelling around the hemisphere twice before the wave energy diminishes around 25 June. The implied group velocity, with

which the wave energy is transmitted, is much faster than the phase velocity of individual waves. An examination of a similar Hovmöller diagram of 500 hPa height anomalies filtered to retain only wavenumbers 1-3 (not shown) reveals no such phase propagation or downstream development associated with these waves.

Summary and concluding remarks

The southeastern part of Australia experienced a prolonged episode of unusually cold weather during May-June 2000. This cold episode was made up of three distinct cold outbreak events in quick succession, between 26 May and 13 June 2000. Of these three cold events, the first and most intense occurred on 27 May, with a maximum temperature in Melbourne of only 10.2°C. The other two events, occurring on 5 June and 12 June 2000, had maximum temperatures slightly higher than that of the first event. In this paper, we have examined, among other things, the synoptic situations leading to the cold outbreak events, along with the associated upper-level circulation features. The changes in track and strength of the participating anticyclones during their lifecycles, and the temporal development of the planetary-scale wave field in both physical and wavenumber space were also studied.

The synoptic situation associated with the major event of 27 May is characterised by the presence of an anticyclone-cyclone pair south of Australia, reminiscent of the 'classic'-type outbreak events found in some previous investigations (Perrin and Simmonds 1995; Simmonds and Richter 2000). On the onset day, the configuration of the anticyclone-cyclone pair and their positioning relative to southeast Australia were suggestive of a strong northward advection of very cold air from continental Antarctica. This result is confirmed by calculating six-day backward trajectories of air parcels arriving at Melbourne for each day of a period surrounding the cold outbreak day. Consistent with the suggestion of Simmonds and Richter (2000), the behaviour of the anticyclones during the cold episode is found to be more instrumental than that of the companion cyclone.

The fact that the anticyclonic systems featured prominently during the cold episode led us to examine some further aspects of the systems in detail. In particular, the time development of the systems' movement, intensity, height, and effective radius were studied quantitatively. It was found that the onsets of two of the three cold events in the MJ2000 episode coincided with the arrival of anticyclones at the Australian sector. These anticyclones were particular-

ly long-lived (21 and 17 days) compared to typical anticyclone lifecycles and travelled a long distance over the Southern Indian Ocean before decaying near Australia. Leading up to the cold events, these anticyclones were very intense, large, and 'high'.

During the MJ2000 episode, hemispheric distributions of anomalous height field exhibited considerable wave-like organisation. This was particularly pronounced at middle and upper tropospheric levels. To investigate the possible relationship between this planetary-scale organisation and the cold outbreaks in the Australian region, aspects of the 500 hPa height anomalies were examined in both the physical and wavenumber spaces. A significant increase in wave amplitudes was indeed found in the Australian sector before the onsets of the cold outbreaks. This increase was mostly contributed by wavenumber 4. Shortly before the onset of each cold outbreak in the MJ2000 episode, wavenumber 4 experienced a marked amplification, followed by a temporary decay for a brief period. It was during this decay period that the cold outbreaks took place.

Considering the central role played by wavenumbers 4 and 5, we filtered the height anomalies, retaining only wavenumbers 4 and 5, to have a closer look at the longitude-and-time development of the amplitudes and phases of these waves. The wave amplification and the eastward phase propagation are now more clearly seen to occur during the cold events of 27 May and 12 June in the Australian sector. A careful examination of the longitude-time plot reveals that significant downstream development of the wave group takes place over a period covering the MJ2000 episode. It is also seen that the eastward propagation of the wave energy associated with the downstream wave development played a significant role in initiating two of the three cold outbreak events in southeast Australia during the MJ2000 episode. No such obvious connection was, however, found for the cold event of 5 June, suggesting that a different mechanism may have operated during this event.

It is clear from the above results that the same two cold outbreak events were related to the downstream energy propagation and the two long-lived anticyclones. This is perhaps not surprising as the anticyclones may well be parts of the wave group exhibiting the downstream development. That this was indeed the situation is apparent in the case of the anticyclone associated with the cold event of 27 May, as seen in the longitude-time plot of height anomalies at 55°S. In a more general context, links between the synoptic developments of weather over southern Australian and downstream energy propagation were emphasised in a number of previous studies (e.g., Noar 1973; Stern 1980). One somewhat unusual result of

the present study is that the downstream wave development was not continuous in longitude. Rather, the energy containing, large-amplitude wave train initially covered the entire eastern hemisphere. Subsequently, the wave energy transmitted rapidly to the western hemisphere, resulting in an amplified wave train there. It is, however, not clear whether such a discontinuous energy propagation is an artifact of filtering of the height anomalies. If it proves to be a real atmospheric phenomenon, then it is worthwhile to understand this unexpected feature of the downstream energy propagation, as the latter process is shown to be so closely related to cold outbreaks. Another unusual characteristic of the downstream development in the MJ2000 event is its very long lifetime. It is of interest to see what mechanism led to such a long and almost uninterrupted downstream energy propagation, making two revolutions around the hemisphere.

References

- Bluestein, H.B. 1992. *Synoptic-dynamic Meteorology in Midlatitudes, Vol. 1*. Oxford University Press, New York, 431 pp.
- Boyle, J.S. 1986. Comparisons of the synoptic conditions at midlatitudes accompanying cold surges over east Asia for the months of December 1974 and 1978. Part I: Monthly mean fields and individual events. *Mon. Weath. Rev.*, *114*, 903-30.
- Colle, B.A. and Mass, C.F. 1995. The structure and evolution of cold surges east of the Rocky Mountains. *Mon. Weath. Rev.*, *123*, 2577-610.
- Fortune, M.A. and Kousky, V.E. 1983. Two severe freezes in Brazil: Precursors and synoptic evolution. *Mon. Weath. Rev.*, *111*, 181-96.
- Garreaud, R.D. 2000. Cold-air incursions over subtropical South America: Mean structure and dynamics. *Mon. Weath. Rev.*, *128*, 2544-59.
- Hannay, A. 1960. Cold outbreaks in southern Australia in relation to sub-Antarctic circulations. *Antarctic Meteorology*. Melbourne: Pergamon Press, 153-75.
- Hovmöller, 1949. The trough-and-ridge diagram. *Tellus*, *1*, 62-6.
- Jones, D.A. and Simmonds, I. 1993. A climatology of Southern Hemisphere cyclones. *Climate Dyn.*, *9*, 131-45.
- Jones, D.A. and Simmonds, I. 1994. A climatology of Southern Hemisphere anticyclones. *Climate Dyn.*, *10*, 333-48.
- Joung, C.H. and Hitchman, M.H. 1982. On the role of successive downstream development in East Asian polar outbreaks. *Mon. Weath. Rev.*, *116*, 1224-37.
- Kalnay, E. and coauthors 1996. The NCEP/NCAR 40-year Reanalysis project. *Bull. Am. met. Soc.*, *77*, 437-71.
- Kistler, R., Kalnay, E., Collins, W., Saha, S., White, G., Woollen, J., Chelliah, M., Ebisuzaki, W., Kousky, V., van den Dool, H., Jenne, R. and Fiorino, M. 2001. The NCEP-NCAR 50-yr reanalysis: Monthly means CD-ROM and documentation. *Bull. Am. met. Soc.*, *82*, 247-67.
- Konrad, C.E. 1996. Relationships between the intensity of cold air outbreaks and the evolution of synoptic and planetary scale features over North America. *Mon. Weath. Rev.*, *124*, 1067-83.
- Konrad, C.E. 1998. Persistent planetary scale circulation patterns and their relationship with cold air outbreak activity over the eastern United States. *Int. J. Climatol.*, *18*, 1209-21.
- Konrad, C.E. and Culocci, S.J. 1989. An examination of extreme cold air outbreaks over eastern North America. *Mon. Weath. Rev.*, *117*, 2687-700.
- Krishnamurti, T.N., Tewari, M., Chakraborty, D.R., Marengo, J., Silva Dias, P.L. and Satyamurty, P. 1999. Downstream amplification: A possible precursor to major freeze events over south eastern Brazil. *Weath. forecasting*, *14*, 242-70.
- Lagouvardos, K., Kotroni, V. and Kallos, G. 1998. An extreme cold surge over the Greek peninsula. *Q. Jl. R. met. Soc.*, *124*, 2299-327.
- Law, R. 1993. Modelling the global transport of atmospheric constituents. Ph.D. thesis, School of Earth Sciences, University of Melbourne, 204 pp.
- Marengo, J., Cornejo, A., Satyamurty, P., Nobre, C. and Sea, W. 1997. Cold surges in tropical and extratropical South America. *Mon. Weath. Rev.*, *124*, 2759-86.
- Murray, R.J. and Simmonds, I. 1991. A numerical scheme for tracking cyclone centres from digital data. Part I: Development and operation of the scheme. *Aust. Met. Mag.*, *39*, 155-66.
- Noar, P.F. 1973. Energy dispersion and other features of the middle latitude circulation in the Australian region. *Met. Study*, *24*, AusInfo, Canberra, 96 pp.
- Orlanski, I. and Sheldon, J.P. 1995. Stages in the energetics of baroclinic systems. *Tellus*, *47A*, 605-28.
- Pagowski, M. and Moore, G.W.K. 2001. A numerical study of an extreme cold-air outbreak over the Labrador Sea: Sea ice, air-sea interaction, and development of polar lows. *Mon. Weath. Rev.*, *129*, 47-72.
- Perrin, G. and Simmonds, I. 1995. The origin and characteristics of cold-air outbreaks over Melbourne. *Aust. Met. Mag.*, *44*, 41-59.
- Pook, M.J. 1992. An icy blast over southern Australia – was there an Antarctic connection? *ANARE News*, *69*, 16-17.
- Roggers, J.C. and Rohli, R.V. 1991. Florida citrus freezes and polar anticyclones in the Great Plains. *Jnl climate*, *4*, 1103-13.
- Schultz, D.M., Bracken, W.E., Bosart, L.F., Hakim, G.J., Bedrick, M.A., Dickinson, M.J. and Tyle, K.R. 1997. The 1993 superstorm cold surge: Frontal structure, gap flow, and tropical impact. *Mon. Weath. Rev.*, *125*, 5-39.
- Schultz, D.M., Bracken, W.E. and Bosart, L.F. 1998. Planetary- and synoptic-scale signatures associated with central American cold surges. *Mon. Weath. Rev.*, *126*, 5-27.
- Seaman, R., Steinle, P. and Hart, T. 1993. The impact of manually derived Southern Hemisphere sea level pressure data upon forecasts from a global model. *Weath. forecasting*, *8*, 363-8.
- Simmonds, I., Murray, R.J. and Leighton, R.M. 1999. A refinement of cyclone tracking methods with data from FROST. *Aust. Met. Mag.*, *Special Issue*, 35-49.
- Simmonds, I. and Keay, K. 2000. Mean Southern Hemisphere extratropical cyclone behaviour in the 40-year NCEP-NCAR Reanalysis. *Jnl climate*, *13*, 873-85.
- Simmonds, I. and Richter, T. 2000. Synoptic comparison of cold events in winter and summer and in Melbourne and Perth. *Theor. Appl. Climatol.*, *67*, 19-32.
- Stern, H. 1980. An interesting example of downstream development. *Meteorological Note 111*, Bur. Met., Australia, 18 pp.
- Taylor, C.M. and Stern, H. 1982. A cold outbreak Over Victoria - 31 May 1977. *Meteorological Note 130*, Bur. Met., Australia, 35 pp.
- Vera, C.S. and Vighiarolo, P.K. 2000. A diagnostic study of cold-air outbreaks over South America. *Mon. Weath. Rev.*, *128*, 3-24.
- Wu, M.C. and Chan, J.C.L. 1997. Upper level features associated with winter monsoon surges over South China. *Mon. Weath. Rev.*, *125*, 317-40.
- Xue, H.J., Pan, Z.Q. and Bane, J.M. 2000. A 2D coupled atmosphere-ocean model study of air-sea interactions during a cold air out-

break over the Gulf Stream. *Mon. Weath. Rev.*, 128, 973-96.